Hydrophobic Core Substitutions in Calbindin D_{9k}: Effects on Stability and Structure†

Karin Julenius,* Eva Thulin, Sara Linse, and Bryan E. Finn*

Physical Chemistry 2, Chemical Center, Lund University, P.O. Box 124, S-221 00 Lund, Sweden

Received October 24, 1997; Revised Manuscript Received March 13, 1998

ABSTRACT: The effects of hydrophobic core mutations on the stability and structure of the four-helix calcium-binding protein, calbindin D_{9k}, have been investigated. Eleven mutations involving eight residues distributed within the hydrophobic core of calbindin D_{9k} were examined. Stabilities were measured by denaturant and thermal induced unfolding monitored by circular dichroism spectroscopy. The mutations were found to exert large effects on the stability with midpoints in the urea induced unfolding varying from 1.8 M for Leu23 → Gly up to 6.6 M for Val70 → Leu and free energies of unfolding in the absence of denaturant ranging from 6.6 to 27.4 kJ/mol for the Phe66 → Ala mutant and the wild-type, respectively. A significant correlation was found between the difference in free energy of unfolding ($\Delta\Delta G_{NU}$) and the change in the surface area of the side chain caused by the mutation, in agreement with other studies. Notably, both increases and decreases in side-chain surface area caused quantitatively equivalent effects on the stability. In other words, a correlation between the absolute value of the change in the surface of the side chain and $\Delta\Delta G_{NU}$ was observed with a value of approximately 0.14 kJ M^{-1} $Å^{-2}$. The generality of this observation is discussed. Significant effects on the cooperativity of the unfolding reaction were also observed. However, a correlation between the cooperativity and $\Delta\Delta G_{NU}$, which has been reported in other systems as an indication of effects of mutations on the unfolded state, was not observed for calbindin D_{9k}. Despite the large effects on $\Delta\Delta G_{NU}$ and cooperativity, the structures of the mutants in the native form remained intact as indicated by circular dichroism, NMR, and fluorescence measurements. The structural response to calcium-binding was also conserved. The following paper in this issue [Kragelund, B. B., et al. (1998) *Biochemistry 37,* 8926−8937] examines the effects of these mutations on the calcium binding properties of calbindin D_{9k}.

Recent advances in the field of protein engineering have demonstrated that the ability to rationally design structures, or at least folds, is now a reality (*2, 3*). The importance of noncovalent interactions in determining the highly specific structures of proteins has long been a subject of experimental and theoretical study and continues to grow at a brisk pace (*4*−*6*). The four-helix bundle motif has been a particularly attractive model system due to its relative simplicity as well as its common occurrence among a wide range of proteins. A notable example of its use in protein engineering studies is the work of Degrado and co-workers who demonstrated one of the first de novo approaches to protein design (*7, 8*).

The four-helix bundle domain is a commonly occurring fold in which the amphipathic helices pack against one another to form a hydrophobic core of nonpolar residues from all four helices. The polar residues on the outer sides of the helices decorate the surface of the domain and solubilize it. Functional sites are often found at the loops connecting the helices, as for example within the calmodulin superfamily of EF-hand proteins where two calcium ions are bound in two loops on the same end of the bundle (*9, 10*). The four-helix bundle fold allows for extensive changes in tertiary packing to occur without significant change in the secondary structure. A striking example is calmodulin itself which contains two globular domains of the four-helix bundle type connected by a flexible linker. Each domain is a bundle of four antiparallel helices comprising the two EF-hand subdomains. The two loops between helices 1 and 2 and helices 3 and 4 contain the calcium-binding sites. Small local conformational changes in the sites where calcium is bound are propagated to substantially larger rearrangements at the other end of the bundle resulting in exposure of a large hydrophobic surface. This response to calcium binding involves changes in interhelix angles which open a binding site for enzymes that are regulated by calmodulin.

The four-helix bundle fold can also prove resistant to conformational change, as in calbindin D_{9k}, which contains one domain of two EF-hands. In this case, calcium binding at one end of the bundle causes only subtle conformational changes in the bundle and no increase in the exposure of hydrophobic surface. Like other proteins of this class, the calcium-binding ligands are arrayed around the loops in the EF-hand motif and coordinate the calcium ion in a pentagonal bipyrimidal geometry (*9, 10*). In the second site, most ligands are contributed from carboxyl ligands of aspartic and

† This work was initiated under a grant by the U.S. Public Health Service (GM 14691 to B.E.F.) and was also supported by the Swedish Natural Science Research Foundation (K10178−305 to S.L.) and the Swedish Foundation for Strategic Research (to B.E.F.).

* To whom correspondence should be addressed. E-mail: Karin.Julenius@fkem2.lth.se, Bryan.Finn@fkem2.lth.se. Tel: +46-46-222-8254. Fax: +46-46-222-4543.

S0006-2960(97)02642-1 CCC: $15.00
Published on Web 05/30/1998

glutamic acid side chains with the last being a bidentate Glu ligand. The first site contains a two residue insertion which leads to an alteration of the loop conformation. This causes the calcium ion to be liganded by the backbone carbonyls instead of the side-chain carboxyls with the exception of the final bidentate Glu ligand which remains coordinated. Site 1 is therefore referred to as a "pseudo-EF-hand". The possibility that this feature distinguishes the sensor vs buffer behaviors of calbindin D_{9k} and calmodulin was disproved in an extensive study of re-engineering the pseudo-EF-hand into a normal EF-hand (*11*, *12*). It was shown that a calbindin D_{9k} with two standard EF-hands retained the structure and calcium-binding response of the wild-type protein. Calbindin D_{9k} has no disulfide bonds and a high surface charge density; 27 of its 75 residues are charged at neutral pH, and the net charge is −7. This leads to significant destabilizing charge−charge repulsions (*13*) in the apo form; however, the protein is extremely stable ($T_m \approx 85$ °C) (*14*) pointing to important contributions to the stability from the core residues that more than compensate for the electrostatic repulsions. Another demonstration of the well-packed hydrophobic core of calbindin D_{9k} is that the two subdomains produced by cleavage of the linker loop between the two EF-hands form heterodimers when mixed in the presence of Ca^{2+} reconstitute the intact structure (*15*). In its Ca^{2+}-bound state, it is resistant to thermal denaturation and stays folded in 10 M urea. Only the apo state of the protein is therefore amenable to mutational analysis of protein stability.

The present study attempts to understand the subtle interplay of forces that regulate the structure and function evolved by naturally occurring proteins, in this case proteins of the EF-hand family of calcium-binding proteins. In comparing calbindin D_{9k} to calmodulin, one finds that calbindin D_{9k} shares 23 and 30% absolute identity with the N- and C-terminal domains of calmodulin, respectively (also called TR_1C and TR_2C), and 54 and 57% homology with respect to residue type (nonpolar, negatively charged, etc.). Yet despite these similarities, as noted, there are large differences in their conformational response to the binding of calcium and therefore their roles in vivo. Calmodulin, which undergoes a conformational change to open a binding site, is knows to act as an activator of a large number of target proteins (*16*). The exact function of calbindin D_{9k} is less clear, but available evidence indicates that it acts in a capacity in calcium homeostasis.

In this study, we characterize the effect of mutations of hydrophobic amino acids on the structural and folding properties of calbindin D_{9k}. The paper examines the effects of these mutations on the stability of the protein and analyzes these effects in relation to other calcium-binding proteins as well as proteins of other classes. Through site-directed mutagenesis, we have made 11 single mutations at eight sites in the hydrophobic core of calbindin D_{9k} (Figure 1). The free energy of unfolding by urea, ΔG_{NU}, has been measured by circular dichroism (CD)[1] spectroscopy of the apo forms of these mutants along with the wild-type protein. We compare our results to earlier studies of hydrophobic mutants involving other proteins and investigate the correlations between change in stability, $\Delta\Delta G_{NU} = \Delta G_{NU}(mut) - \Delta G_{NU}(wt)$, and other factors. The mutations resulted in decreased $\Delta G_{NU}(H_2O)$ of up to 21 kJ/mol. No stabilizing mutations were found. The thermal unfolding as measured by circular dichroism shows an apparent discrepancy from an earlier DSC study. Structural changes of the mutants and changes in their structural response to calcium binding was measured by binding of the hydrophobic fluorescent dye, ANS. Neither the wild-type nor any of the mutants exhibited a calcium-dependent affinity for ANS, as has been observed for calmodulin (*17*, *18*). In cases where the native structure of the least stable mutants were possibly changed, NMR and CD spectroscopy were used to confirm their structural integrity. The following paper in this issue (*1*) examines the effects of hydrophobic mutations on the functional properties of calbindin D_{9k} such as calcium binding and kinetics.

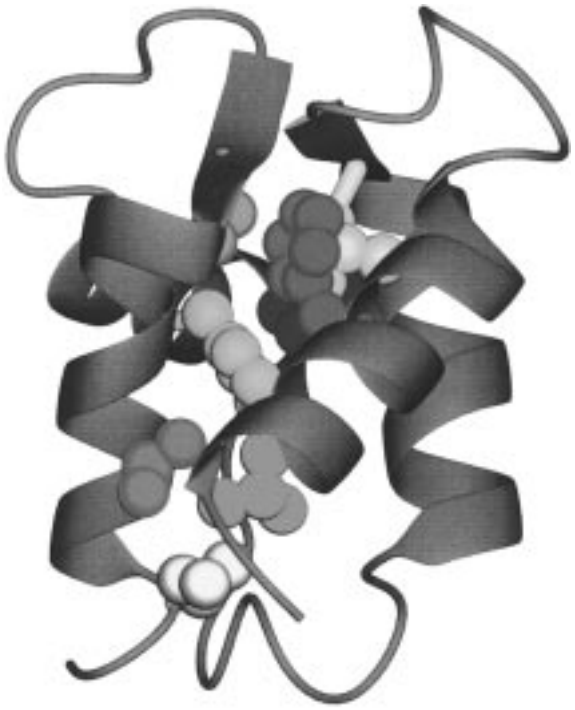

FIGURE 1: Ribbon drawing showing the locations of core hydrophobic residues of bovine calbindin D_{9k} examined in this study. Leu6 is shown in red, Phe10 in magenta, Leu23 in yellow, Leu28 in blue, Val61 in cyan, Phe66 in orange, Val70 in green, and Ile73 in white. This figure was made with the programs MOLMOL (*75*) and POVRAY (©1997; The POVRAY Team) from coordinates of the solution structure of apo-calbindin D_{9k} determined by NMR spectroscopy (*74*) (Protein Data Bank filecode 1clb).

MATERIALS AND METHODS

Protein Mutagenesis. The mutant proteins derived from bovine calbindin D_{9k} were synthesized, expressed in *Escherichia coli*, and purified as described previously (*19*, *20*).

[1] Abbreviations: CD, circular dichroism; NMR, nuclear magnetic resonance; DSC, differential scanning calorimetry; EDTA, ethylendiaminetetraacetic acid; Tris, tris(hydroxymethyl)aminomethane; SDS, sodium dodecyl sulfate; COSY, correlated spectroscopy; NOESY, nuclear Overhauser enhancement spectroscopy; TOCSY, total correlation spectroscopy; ANS, 8-anilino-1-naphthalenesulfonic acid; P43M, calbindin D_{9k} mutant with the substitution Pro43 → Met. All other mutants contain the Pro43 → Met substitution plus the substitutions as follows: L6V, Leu6 → Val; F10A, Phe10 → Ala; L23A, Leu23 → Ala; L23G, Leu23 → Gly; L28A, Leu28 → Ala; V61A, Val61 → Ala; V61G, Val61 → Gly; F66A, Phe66 → Ala; F66W, Phe66 → Trp; V70L, Val70 → Leu; I73V, Ile73 → Val.

Table 1: Fraction Solvent-Accessible Surface Area of the Mutated Amino Acid Residues in Calbindin D_{9k}

	fraction exposed area[a] (%)	
residue	total	side chain
Leu6	6	8
Phe10	0	0
Leu23	0	0
Leu28	1	1
Val61	0	0
Phe66	1	1
Val70	8	10
Ile73	40	37

[a] Solvent accessible surface area of the residues in question in apo calbindin D_{9k} divided by their accessible surface area in extended conformation as calculated with NACCESS (Hubbard & Thorton, 1993). The results are median values from 33 solution structures determined by NMR spectroscopy (*74*) (Protein Data Bank filecode 1clb).

The purity was confirmed by agarose gel electrophoresis in the presence of 1 mM EDTA or 2 mM $CaCl_2$, SDS−polyacrylamide gel electrophoresis, isolelectric focusing, and ^{1}H NMR spectroscopy. The residual calcium content was determined using chromophoric Ca^{2+} chelators and UV absorbance spectroscopy as well as by ^{1}H NMR spectroscopy.

The reference protein, referred to as the wild-type, is the minor-A form of bovine calbindin D_{9k} with two modifications. The first is a methionine residue added at the N-terminus for expression purposes. The second is the mutation P43M which eliminates the complication of multiple native forms due to cis−trans isomerism of this proline residue as observed previously (*21*). All other mutants are referred to with their mutation relative to this reference form.

The mutants examined in this study are L6V, F10A, L23A, L23G, L28A, V61A, V61G, F66W, F66A, V70L, and I73V. The mutated amino acid residues are interspersed throughout the various elements of secondary structure, and all participate in the central hydrophobic core of calbindin D_{9k} (Figure 1). Their relative exposed surface areas are summarized in Table 1.

Solutions. All chemicals were of the highest grade commercially available. The urea was of Aristar quality from BDH (Dorset, England). Lyophilized protein was dissolved in 1 mL of buffer to give protein stock solutions of 1 mM, which were diluted to give protein concentrations of 20 μM. Protein concentrations were confirmed by acid hydrolysis and amino acid analysis. The buffer used in all apo experiments was 10 mM potassium phosphate, pH 7.0, with 0.5 mM EGTA. Fresh 9 or 10 M urea solution, pH 7.0, containing 10 mM potassium phosphate and 0.5 mM EGTA was prepared every day. The buffer and the urea solutions were mixed in varying proportions to give samples with urea concentrations ranging from 0 to 9.8 M and an exact amount of protein stock solution was added to each. For the calcium addition experiment, 2 mM Tris/HCl buffer, pH 7.5, was used. After recording the first spectra, 10 μL of 50 mM $CaCl_2$ was added to 490 μL of the protein sample solution and a new spectra was recorded.

Data Collection. All CD spectra were obtained using a Jasco J-720 spectropolarimeter with a Jasco PTC-343 Peltier type thermostatic cell holder. Quartz cuvettes with a path length of 1 mm were used. All data except the thermal unfolding curves were collected at 25.0 °C. For the urea unfolding measurements, the CD spectra were recorded between 205 and 250 nm. The CD signals at 222 nm were measured after subtraction of the background buffer spectra. All spectra for a specific mutant were run on the same day. For the investigations of the possibly partly unfolded mutant F66A, CD spectra were recorded between 185 and 250 nm and the buffer spectra were subtracted. For the thermal unfolding, quartz cuvettes with Teflon stoppers were used. The cuvettes were completely filled to prevent concentration changes due to evaporation. The ellipticity at 222 nm was measured as the temperature was raised from 3.0 to 90.0 °C and decreased to 3.0 °C at a rate of 50 °C/h.

Fluorescence spectra were collected on a Spex Fluorolog fluorescence spectrometer. For ANS-binding studies, ANS and apo protein stocks were mixed in a 1:1 ratio at 20 μM and spectra were recorded using an excitation wavelength of 350 nm and emission was measured between 400 and 550 nm. For tryptophan fluorescence measurements, an excitation wavelength of 295 nm was used while emission was measured between 300 and 500 nm.

For NMR studies, samples of wild-type and F66A calbindin D_{9k} were prepared in self-buffered solutions of 90% H_2O/10% D_2O at a protein concentration of 3 mM, pH 6.0. All spectra were recorded at a temperature of 300 K. One-dimensional spectra and two-dimensional COSY, TOCSY, and NOESY (*22*−*24*) spectra for the F66A mutant were collected on a GE Omega NMR spectrometer operating at 500.12 MHz for ^{1}H. Spectral data was processed and analyzed using the Felix software package (Molecular Simulations Inc.) using standard methods.

Data Analysis. The mean residue ellipticity $[\Theta]_{MRW}$ (deg cm^2/dmol) is calculated from measured ellipticity Θ (degrees) using the following equation:

$$[\Theta] = \frac{\Theta 100}{cd} \tag{1}$$

where c is the concentration in molarity and d is the path length in centimeters.

The CD data were analyzed with the software KaleidaGraph (Synergy Software) for Macintosh and fitted to a linear extrapolation model assuming two-state unfolding as previously described (*25*). The baselines before and after the actual unfolding were fitted to the straight lines

$$Y_N = k_N[D] + b_N \tag{2a}$$

$$Y_U = k_U[D] + b_U \tag{2b}$$

where k_N and k_U are the slopes, b_N and b_U are the intercepts, and [D] is the denaturant concentration (Figure 2). The data have been normalized according to

$$F_{app} = (Y_O - Y_N)/(Y_U - Y_N) \tag{3}$$

where Y_O is the observed ellipticity at 222 nm (Figure 2). F_{app} is fitted to

$$F_{app} = \frac{e^{-(\Delta G_{NU}(H_2O) - m_D[D])/RT}}{1 + e^{-(\Delta G_{NU}(H_2O) - m_D[D])/RT}} \tag{4}$$

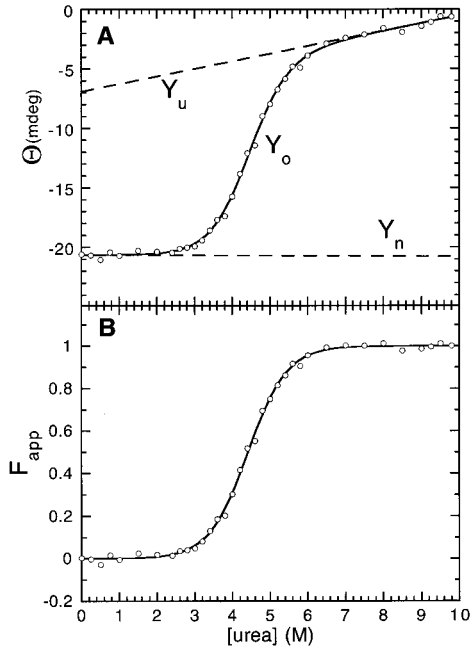

FIGURE 2: The unfolding of I73V calbindin D_{9k} as a function of urea concentration, [urea], measured at 25.0 °C using circular dichroism at 222 nm. (A) The ellipticity, Θ, before normalization. The solid line, Y_o, shows the best fit of eq 5 and the dashed lines show the baselines before, Y_n, and after, Y_u, unfolding resulting from the fit. (B) The fraction of unfolded protein, F_{app}, normalized according to eq 3. The solid line shows the best fit of eq 4 to the data.

where $\Delta G_{NU}(H_2O)$ is the unfolding free energy in pure water, m_D is the influence of denaturation concentration on the stability, R is the molar gas constant, and T is the temperature. The free energy toward unfolding by urea, ΔG_{NU}, is assumed to obey the linear equation $\Delta G_{NU} = \Delta G_{NU}(H_2O) - m_D[D]$. To find the best possible fit of all six parameters and to evaluate the errors in a consistent way, they were all optimized simultaneously using the equation

$$Y_O = \frac{(k_N[D] + b_N) + (k_U[D] + b_U)e^{-(\Delta G_{NU}(H_2O) - m_D[D])/RT}}{1 + e^{-(\Delta G_{NU}(H_2O) - m_D[D])/RT}} \quad (5)$$

Due to the lack of sufficient data points defining Y_N of F10A and F66A and Y_U of F66W and V70L, the calculated slopes of these baselines (k_N and k_U, respectively) are regarded as unreliable. They were, therefore, instead fixed to the mean slopes resulting from the fittings of the other mutants, and new fits for these mutants only including the five other parameters [b_N, k_U, b_U, $\Delta G_{NU}(H_2O)$, m_{urea} for F10A and F66A; and k_N, b_N, b_U, $\Delta G_{NU}(H_2O)$, m_{urea} for F66W and V70L] were made. When calculating the mean slopes [k_N(mean) and k_U(mean)], the slope values were weighted with respect to their standard deviations (σ) according to

$$k_U^{mean} = \frac{\sum_{mutants} \frac{k_U}{\sigma_{k_U}}}{\sum_{mutants} \frac{1}{\sigma_{k_U}}} \quad (6a)$$

$$k_N^{mean} = \frac{\sum_{mutants} \frac{k_N}{\sigma_{k_N}}}{\sum_{mutants} \frac{1}{\sigma_{k_N}}} \quad (6b)$$

The resulting means of the slopes were -0.38 ± 0.12 for k_u and 0.09 ± 0.43 for k_n. The errors in the reported values of the different parameters were estimated to 1 standard deviation. The standard deviations were obtained directly from the fitting procedures. Since the data for F10A, F66A, F66W, and V70L were only fit with five of the six parameters, the errors in these cases are probably underestimated. C_M is defined according to

$$C_M = \Delta G_{NU}(H_2O)/m_D \quad (7)$$

For the thermal unfolding, Y_U was beyond the range of accessible temperature in all cases. For normalization and comparison of the curves, Y_U was set to be equal to b_U obtained for the urea unfolding. Y_N was fit using linear regression to the points defining the first, flat part of the curve. F_{app} was calculated using eq 3.

In the comparison of our results to data obtained in previous studies of other proteins, only single-site mutations involving the exchange of one hydrophobic residue for another were used. Thus, the residues tryptophan, phenylalanine, isoleucine, leucine, methionine, valine, alanine, and glycine were regarded as applicable. Where the free energy toward unfolding had been measured with different methods and/or under different conditions, the stability measured with the method under the conditions most resembling those of the calbindin D_{9k} study was used. $\Delta\Delta G_{NU}$ is defined as

$$\Delta\Delta G_{NU} = \Delta G_{NU}(\text{mutant}) - \Delta G_{NU}(\text{wild-type}) \quad (8)$$

and $|\Delta m|$ is defined as

$$|\Delta m| = |(m_{mutant} - m_{wild-type})/m_{wild-type}| \quad (9)$$

The errors in the parameters of the straight lines were estimated to be equal to 1 standard deviation. The linear correlations were tested for their significance and the probabilities that the correlations occurred by chance, p, were calculated using standard statistical methods (*26*).

RESULTS

Design of Mutant Proteins. All mutations of calbindin D_{9k} were based on a modified wild-type protein P43M in which a proline previously demonstrated to occur in both cis and trans conformations (*21*) was removed in order to simplify analysis of folding studies. The locations and types of amino acid substitutions that were made were chosen with the aim of sampling the entire hydrophobic core. All types of secondary structure including the four-helix bundle as well as the small β-sheet between the calcium-binding loops were sampled. Residues both close to the surface and completely buried in the core were chosen and the type of mutation was varied to sample both increases and decreases in side-chain volume. The residues chosen for mutation are shown in Figure 1.

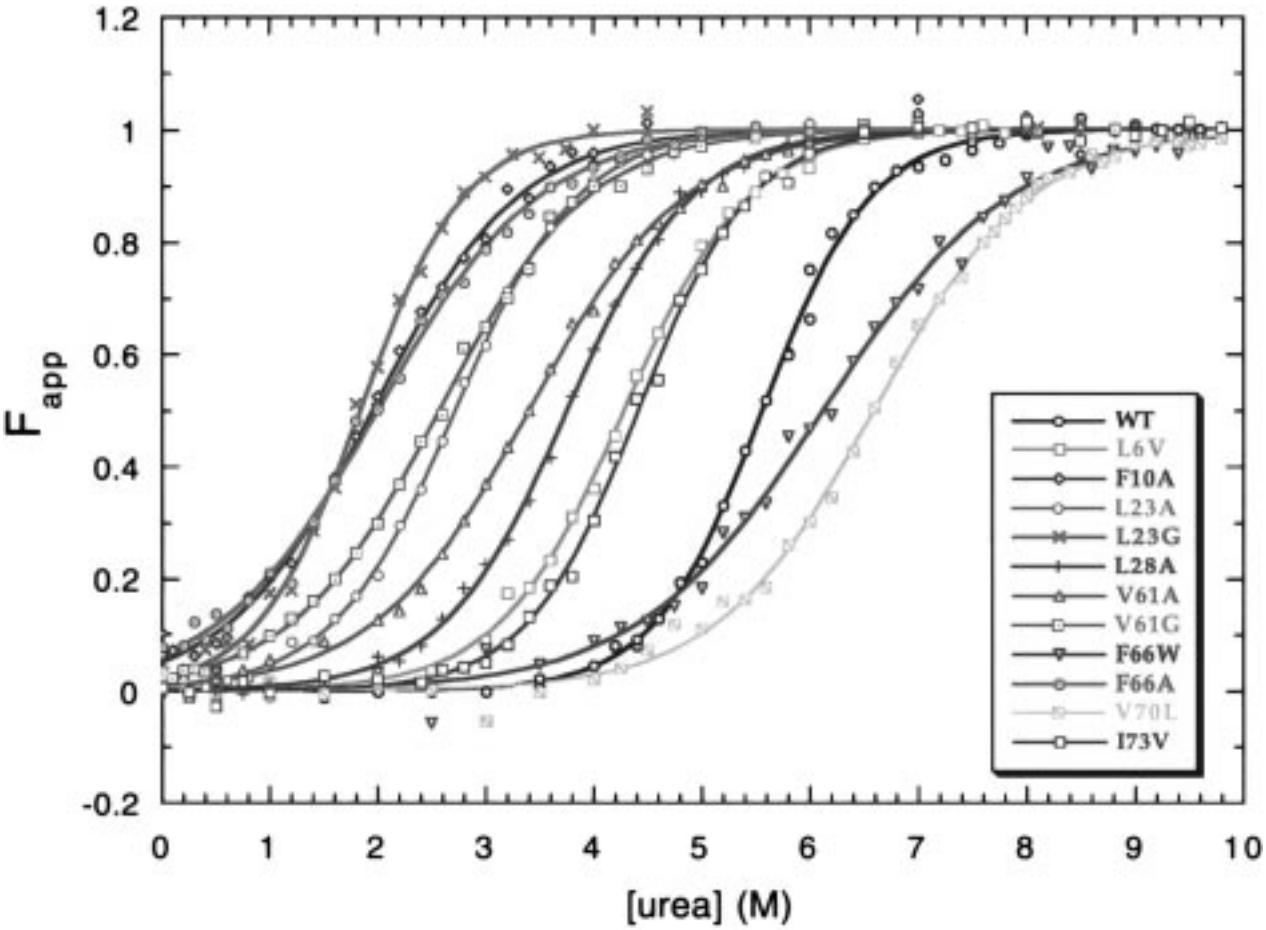

FIGURE 3: The fraction of unfolded protein, F_{app}, for recombinant apo bovine calbindin D_{9k} and engineered mutants as a function of urea concentration. The unfolding was measured at 25.0 °C using circular dichroism at 222 nm and converted to F_{app} as in Figure 2. The mutants are identified by color and symbol in the figure insert.

Table 2: Stability Toward Urea Unfolding of the Calbindin D_{9k} Mutants

	$\Delta G_{NU}(H_2O)$ (kJ mol^{-1})	m_{urea}[a] (kJ mol^{-1} M^{-1})	C_M[b] (M)
wild-type	27.4 ± 1.3	4.9 ± 0.2	5.6
L6V	18.2 ± 1.0	4.2 ± 0.2	4.3
F10A	7.2 ± 0.5	3.7 ± 0.2	2.0
L23A	11.8 ± 0.6	4.3 ± 0.2	2.7
L23G	9.5 ± 1.3	5.1 ± 0.5	1.8
L28A	16.1 ± 0.7	4.3 ± 0.2	3.8
V61A	11.6 ± 0.7	3.4 ± 0.2	3.4
V61G	9.2 ± 0.8	3.6 ± 0.2	2.6
F66W	17.6 ± 1.4	2.9 ± 0.2	6.1
F66A	6.6 ± 0.5	3.3 ± 0.2	2.0
V70L	22.4 ± 1.0	3.4 ± 0.1	6.6
I73V	21.0 ± 1.1	4.8 ± 0.2	4.4

[a] The linear denaturant dependence in the equation $\Delta G_{NU} = \Delta G_{NU}(H_2O) - m_{urea}$[urea]. [b] The midpoint unfolding concentration.

Stability Effects. The normalized ellipticity at 222 nm as a function of urea concentration for solutions of mutant calbindins is shown in Figure 3. The free energies of unfolding in the absence of denaturant, $\Delta G_{NU}(H_2O)$, and the urea concentrations at the transition midpoint, C_M, are summarized in Table 2. ΔG_{NU} ranges widely from 27.4 kJ mol^{-1} for the wild-type to 6.6 kJ mol^{-1} for the F66A mutant. The extrapolated values of $\Delta G_{NU}(H_2O)$ for the 12 mutants indicate that none of the mutations resulted in an increased stability relative to the wild-type. The mutants V70L (C_M = 6.6 M) and F66W (C_M = 6.1 M) exhibited higher C_M values than the wild-type (C_M = 5.5 M), but the reductions in the slopes of their unfolding transitions led to $\Delta G_{NU}(H_2O)$ values less than the wild-type. The mutant with lowest C_M is L23G with a C_M of 1.8 M. The values of the linear denaturant dependencies, m_{urea}, varied substantially from 2.9 kJ mol^{-1} M^{-1} for F66W to 5.1 kJ mol^{-1} M-1 for L23G.

For two of the least stable mutants, F66A and F10A, the normalization and fitting of the unfolding curves gave nonzero values for the fraction of unfolded protein in the absence of denaturant. This raised the question of whether this was an accurate reflection of the state of the protein or an artifact of the fitting procedure. The structure of the least stable mutant, F66A, was investigated to determine if there was any evidence that it is partially unfolded in the absence of denaturant. We first recorded CD spectra at 25.0 °C for solutions of wild-type and F66A at protein concentrations accurately determined by amino acid analysis. The mean residue ellipticities, $[\Theta]_{MRW}$, were determined and the results are shown in Figure 4. $[\Theta]_{MRW}$ differs slightly between the mutant and wild-type. For F66A, the minima at 209 and 223 nm are more negative $[\Theta]_{MRW}$ as compared to the wild-type especially that at 209 nm, consistent with Ala being a more favorable residue for helix formation than Phe (*27*). Thus, while a slight change in the structure may have been caused by the mutation, there is no net loss of secondary structure. The second test is based on the known fact from a previous study (*14*) that the Ca^{2+}-form of calbindin D_{9k} is

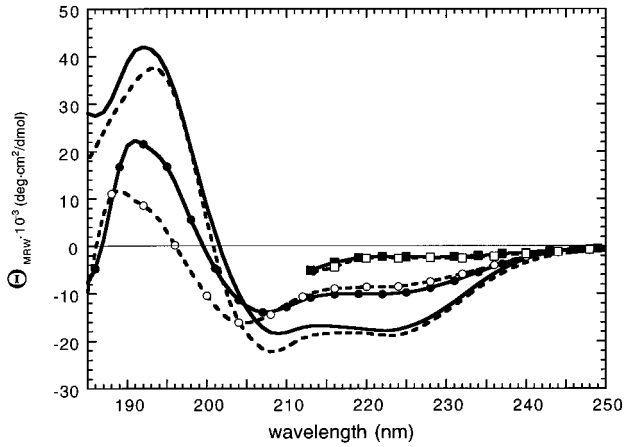

FIGURE 4: The mean residue ellipticity, $[\Theta]_{MRW}$, for wild-type (solid lines) and F66A (dashed lines) calbindin D_{9k} in their apo forms as a function of wavelength. The conditions under which $[\Theta]_{MRW}$ was determined are 25 °C, no urea (no symbols); 90 °C, no urea (open circles); 25 °C, 9 M urea (open squares). Data were collected at 1 nm intervals. Symbols are shown only to distinguish the curves from one another.

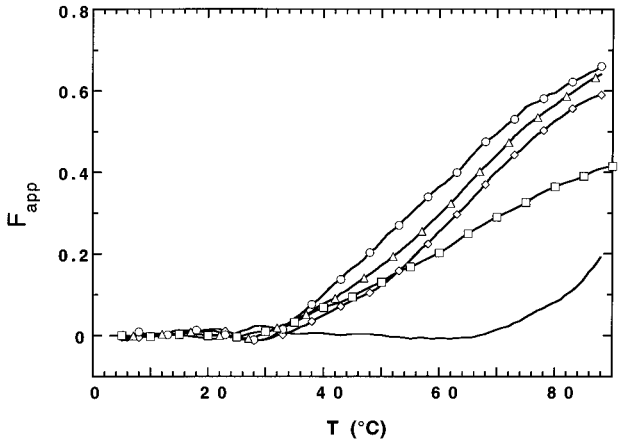

FIGURE 5: The fraction of unfolded protein, F_{app}, for WT (no symbols), F10A (squares), L23G (diamonds), V61G (circles) and F66A (triangles) apo calbindin D_{9k} as a function of temperature. Points were collected at 1 °C intervals while raising the temperature at the rate of 50 °C/h. The unfolding was measured in the absence of urea using circular dichroism at 222 nm. Symbols are shown only to distinguish the curves from one another.

exceptionally stable and is impossible to completely unfold with urea or heat up to 100 °C. It is also known that the ellipticities of the apo- and Ca^{2+}-forms of calbindin D_{9k} differ little due to the fact that calcium-binding induces only subtle changes in the structure. Therefore, any significant calcium-induced changes in the CD spectrum would reflect a stabilization of partially unfolded apo protein toward the fully folded calcium form. We therefore recorded CD spectra of the wild-type and of F66A before and after the addition of $CaCl_2$ in the absence of urea and compared the results. No substantial change in intensities occurred in the ellipticity of the wild-type nor of F66A upon calcium addition, indicating no net increase in the structure of the mutant is induced by calcium binding just as observed for the wild-type. Finally, NMR spectra of the F66A mutant in both the apo and calcium-loaded states were collected. Only minor changes in the pattern of chemical shifts were observed with most differences being less than 0.03 ppm. Those larger than 0.03 ppm were localized to the residues surrounding residue 66 and could be attributed to shielding effects due to the removal of the ring current of phenylalanine upon mutation to alanine. No additional resonances that could be attributed to an unfolded or partially unfolded state in slow exchange with the folded native state were observed (data not shown). Taken together, these results indicate that while the structure of F66A may differ slightly from the wild-type, it exhibits no tendency toward unfolding in the absence of denaturant. While the mean residue ellipticity, $[\Theta]_{MRW}$, variations between wild-type and F66A are not due to changes in the α-helix content based on NMR and calcium-binding data, it has been observed for other calcium-binding proteins such as calmodulin that even changes in the helix−helix angles can give changes in the far-UV CD spectra (*28, 29*). In addition, a theoretical study (*30*) of CD determination of helical content has indicated that great care has to be exercised when conclusions about protein helicity are drawn from CD intensities. Hirst et al. (*30*) propose that the mere fraying of helices, without reduction of the number of helical residues, will significantly reduce the mean residue ellipticity. In addition, effects from the aromatic side chains have been observed to influence the spectra in the far UV (*31*,*32*). Thus, our observations of the changes in $[\Theta]_{MRW}$ due to the F66A mutation are more likely the result of changes in the distribution of microstates in the native form of the less stable F66A mutant which are reflected in a fraying or other dynamic motion in the helices and not a population of partially or fully unfolded states.

Thermal Denaturation. The midpoint temperature of thermal denaturation for wild-type apo calbindin D_{9k} has been determined by calorimetry to be 85 °C (*33*). However, the unfolded baseline lies entirely above 100 °C and is therefore not amenable to thermal denaturation monitored by CD. However, a qualitative comparison of the least stable mutants to the wild-type might shed some light on the effect of these mutants on the thermal stability in relation to the stability measured by denaturant studies. The ellipticity at 222 nm for the apo forms of wild-type, F10A, L23G, V61G, and F66A calbindin D_{9k} was studied as a function of temperature in aqueous solution. A plot of the normalized ellipticities at different temperatures is shown in Figure 5. Surprisingly, even the least stable mutants exhibited similar behavior to the wild-type, namely that they were not completely unfolded at 90 °C. Therefore, the midpoints of thermal denaturation, T_m, and the ΔG_{NU} of the thermal unfolding are difficult to determine quantitatively. It is, however, possible to conclude that the stabilities, ΔG_{NU}, of F10A, L23G, V61G, and F66A calbindin D_{9k} toward thermal unfolding are substantially reduced compared to the wild-type. F10A seems to be more stable than L23G, V61G, and F66A, but apart from that, it is not possible to rank the mutants among themselves. The unfolding of the mutants is surprisingly uncooperative with unfolding transitions ranging over more than 60 °C.

The mean residue ellipticity, $[\Theta]_{MRW}$, was measured for wild-type and F66A at 90.0 °C in phosphate buffer and at 25.0 °C in 9 M urea as well as at 25.0 °C in phosphate buffer to be able to compare the degree of unfolding in the different cases. The results are shown in Figure 4. It is clear from the figure that F66A is more unfolded than wild-type at 90.0 °C, but it is also clear that neither of them are as unfolded at 90.0 °C as they are in 9 M urea.

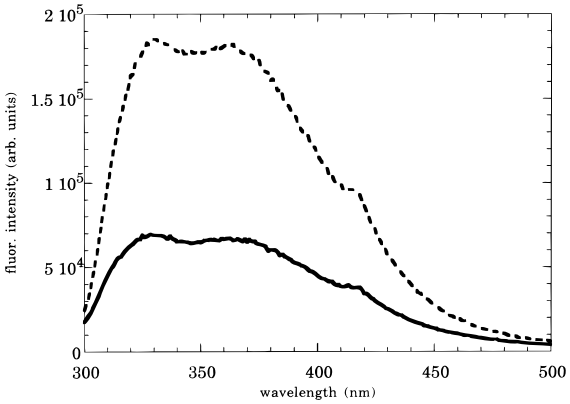

FIGURE 6: Fluorescence emission spectra of the F66W mutant of calbindin D_{9k} in the apo (solid line) and calcium-loaded (dashed line) forms. Tryptophan fluorescence was measured using an excitation wavelength of 290 nm and measuring the emission between 300 and 500 nm with 1 nm step size.

Structural Effects. To investigate the effects of mutations on the structure of calbindin D_{9k}, especially with respect to the conformational response to calcium binding, the degree of exposed hydrophobic surface was measured using the hydrophobic fluorescent dye ANS. This molecule has been widely used as a probe of hydrophobic surfaces on proteins during folding as well as conformational changes, for example in the case of calmodulin (*17, 18*). The fluorescence emission spectrum of free ANS was compared to that in the presence of wild-type calbindin D_{9k} and all mutant calbindins both in their apo and calcium-loaded forms. In all cases, no effect on the spectrum of ANS was observed, neither in the absence nor presence of calcium. This indicates that, despite the large destabilization of the hydrophobic core in many of the mutations studied, none show any indication of the type of calcium-dependent structural changes observed for related proteins such as calmodulin and troponin C.

In a related experiment, the fluorescence spectra of mutant F66W were investigated. By the replacement of Phe66 with a Trp residue, a unique fluorescent probe has been introduced in the central core of calbindin D_{9k}. The fluorescence emission spectra of F66W in the apo and calcium-bound forms are shown in Figure 6. As shown in the figure, the fluorescence of the single Trp residue increases by a factor of 3 upon binding of calcium. This result was surprising since the mutation had a relatively small effect on the stability of the protein and therefore would not have been expected to exhibit calcium-dependent structural changes.

DISCUSSION

Calcium-binding proteins of the EF-hand calmodulin superfamily can be grouped in two categories based on their structural response to calcium binding and, therefore, function. The majority fall into the "sensor" class and are those which, upon binding calcium, undergo a conformational change which allows them to interact with a target and transmit the calcium mediated signal further. This class is exemplified by calmodulin, troponin C, recoverin, and possibly the S100 proteins (*34*). The second class is often referred to as the "buffer" class and includes those which do not undergo a significant conformational change upon calcium binding and who have no well-defined target in vivo. The molecular basis of the difference between these two classes has been the subject of much study but has yet to be resolved conclusively.

Previous studies of the effects of mutations on proteins of the calmodulin superfamily have established the importance of specific residues, especially the calcium ligands and their neighbors, in the function and stability of these proteins (*13, 14, 35, 36*). Attention has especially focused on the bidentate glutamate ligand as a possible trigger for calcium-binding-induced conformational change in calmodulin and troponin C (*35*−*37*). While its importance in the conformational changes of these proteins is well established, the fact that the same bidentate glutamate ligand is found in both sensor-type and buffer-type EF-hand proteins lead us to speculate that other interactions play important roles in distinguishing the calcium-induced conformational response of proteins in the EF-hand superfamily. The goals of the present and accompanying studies are to characterize how mutations in the hydrophobic core of calbindin D_{9k} affect its stability and function.

Stability Effects. Both the stabilities toward unfolding extrapolated to pure water, $\Delta G_{NU}(H_2O)$, and the linear dependencies of the free energies toward unfolding on the denaturant concentration, m_{urea}, of the mutants vary greatly but show no correlation to one another (Figure 3). In general, those mutations causing larger changes in surface area or volume of the side chain gave rise to larger changes in $\Delta G_{NU}(H_2O)$. The correlation is especially evident for those cases where multiple mutations were made of the same residue, such as Leu23 and Val61, which were changed to Ala as well as Gly. A notable set of mutations are those which increased the size of side chains, F66W and V70L. The urea concentrations at the transition midpoint, C_M, of these mutants are substantially higher than for the wild-type, but the free energies of unfolding in pure water, $\Delta G_{NU}(H_2O)$, are substantially lower. This is due to the remarkable decrease in the linear dependencies of the free energy toward unfolding on the denaturant concentration, m_{urea}, and thus the cooperativity of the unfolding reaction.

In an attempt to draw general conclusions about the effects of mutations of hydrophobic amino acid residues on the free energy of unfolding, ΔG_{NU}, and the linear denaturant dependencies, m_D, data were gathered from previous studies. The most well-studied system with regard to hydrophobic mutations is *staphylococcal* nuclease (*38*−*42*). Other examples of proteins for which the changes in ΔG_{NU} due to a number of hydrophobic mutations have been studied are barnase (*43, 44*), sperm whale myoglobin (*45*−*47*), bacteriophage T4 lysozyme (*48*−*53*), bacteriophage f1 gene V protein (*54*), chymotrypsin inhibitor 2 (*55, 56*), and bacteriophage P22 arc repressor (*57*). In Figure 7, we have plotted $\Delta\Delta G_{NU}$ versus the difference in surface area in extended conformation, ΔA (*58*), between mutant and wild-type residues for these proteins. It is obvious from Figure 7 that very large differences in $\Delta\Delta G_{NU}$ can be seen for similar mutations. Few single hydrophobic mutations are stabilizing (positive $\Delta\Delta G_{NU}$). The calbindin D_{9k} data are clearly consistent with results obtained from other proteins. Similar results are obtained when $\Delta\Delta G_{NU}$ is plotted versus the difference in side-chain volume in protein interiors, ΔV (*59*) or versus the difference in free energy of transfer from octanol to water, $\Delta\Delta G_{trans}$ (*60*). The mutations causing a decrease in surface area, volume or hydrophobicity seem to

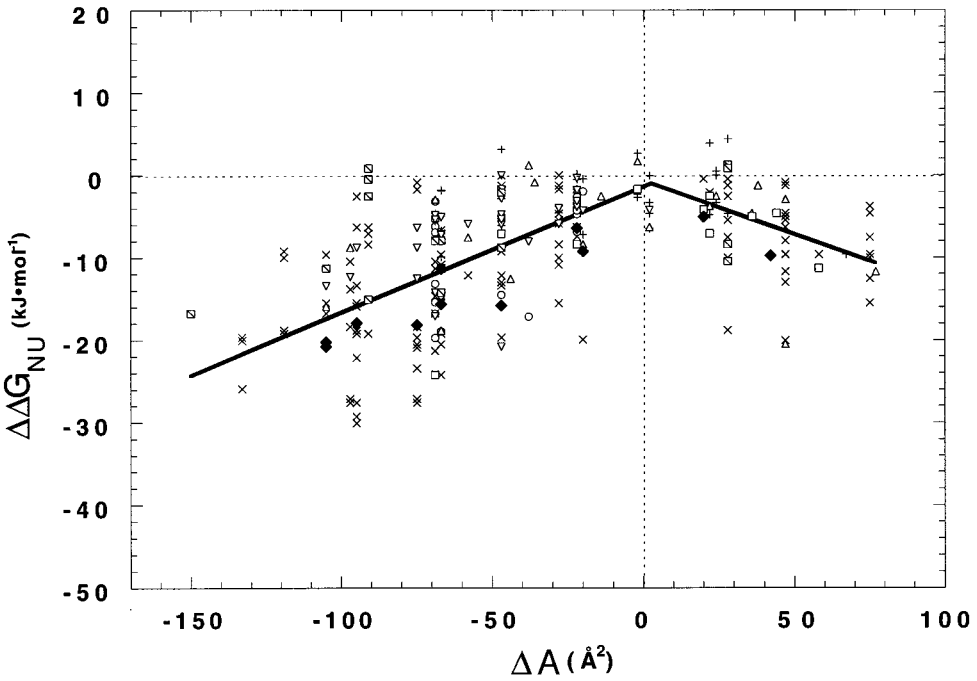

FIGURE 7: The difference in free energy of unfolding, $\Delta\Delta G_{NU}$, as a function of difference in surface area in extended conformation, ΔA, between mutants and the wild-types of bovine calbindin D_{9k} (filled diamonds), *staphylococcal* nuclease (×), barnase (circles), sperm whale myoglobin (+), bacteriophage T4 lysozyme (triangles), bacteriophage f1 gene V protein (squares), chymotrypsin inhibitor 2 (inverted triangles), and bacteriophage P22 arc repressor (squares with slash). $\Delta\Delta G_{NU}$ is defined as $\Delta\Delta G_{NU} = \Delta G_{NU}$(mutant) $- \Delta G_{NU}$(wild-type) and ΔA as $\Delta A = A$(mutant side chain) $- A$(wild-type side chain).

Table 3: Linear Correlations between $\Delta\Delta G_{NU}(H_2O)$[a] and ΔV[b], ΔA[c], and $\Delta\Delta G_{trans}$,[d] Respectively, Calculated by Linear Regression

	$\Delta\Delta G_{NU}$ vs ΔV		$\Delta\Delta G_{NU}$ vs ΔA		$\Delta\Delta G_{NU}$ vs $\Delta\Delta G_{trans}$	
	$\Delta V > 0$	$\Delta V < 0$	$\Delta A > 0$	$\Delta A < 0$	$\Delta\Delta G_{trans} > 0$	$\Delta\Delta G_{trans} < 0$
I[e]	-1.5 ± 0.8	-1.0 ± 0.9	-0.9 ± 0.9	-1.3 ± 0.8	-1.4 ± 1.1	-0.3 ± 0.9
S[e]	-0.12 ± 0.02	0.15 ± 0.01	-0.13 ± 0.02	0.15 ± 0.01	-1.9 ± 0.4	2.1 ± 0.2
correlation	0.58	0.61	0.57	0.63	0.50	0.60

[a] $\Delta\Delta G_{NU}(H_2O)$ values of mutant *staphylococcal* Nuclease, barnase, sperm whale myoglobin, bacteriophage T4 lysozyme, bacteriophage f1 gene V protein, chymotrypsin inhibitor 2, bacteriophage P22 arc repressor and Bovine calbindin D_{9k} are included. [b] The difference in side chain volume in protein interiors (*59*). $\Delta V = V$(mutant side chain) $- V$(wild-type side chain). [c] The difference in surface area in extended conformation (*58*). $\Delta A = A$(mutant side chain) $- A$(wild-type side chain). [d] The difference in free energy of transfer from octanol to water (*60*). $\Delta\Delta G_{trans} = \Delta\Delta G_{trans}$(mutant side chain) $- \Delta\Delta G_{trans}$(wild-type side chain). [e] Constants in the linear equation $\Delta\Delta G_{NU} = I + SX$ (eq 10) where I and S are constants and X is ΔA, ΔV, or $\Delta\Delta G_{trans}$, respectively.

be best treated separately from those causing an increase in surface area, volume, or hydrophobicity. After this distinction was made, straight lines of the form

$$\Delta\Delta G_{NU} = I + SX \qquad (10)$$

(I and S are constants; X is ΔA, ΔV, or $\Delta\Delta G_{trans}$) were calculated using linear regression (Table 3). All of these correlations are statistically highly significant with $p < 0.001$. However, they are far from absolute due to the importance of other factors in the stability. Remarkably, the lines calculated for the mutants resulting in increase in volume, surface area, or hydrophobicity are within experimental error mirror images of the lines for the mutants causing decrease in volume, surface area, or hydrophobicity, i.e., the intercepts are approximately the same and the slopes have the same value, but of opposite sign. Thus, the change in the free energy of unfolding is correlated to the absolute value of the change in the residue surface area with a value of 0.14 kJ M^{-1} $Å^{-2}$. While a correlation in the reduction of side chain and free energies has been noted previously (*43*, *44*, *61*), to our knowledge, this is the first time that increases and decreases are observed to exert equivalent effects on ΔG_{NU}. Notable is also that the intercepts are negative, i.e., mutations changing one residue to another of the same volume, surface area, or hydrophobicity on average lead to destabilization. This result is in line with observations on random point mutations that indicate that in general only one out of 10^3-10^4 mutations will lead to increased protein stability (*62*−*66*). It would appear that most point mutations in the hydrophobic core of a protein will cause a perturbation that can be related to different factors such as ΔA, ΔV, or $\Delta\Delta G_{trans}$ of the mutated residues. The effect of a certain perturbation on the protein is largely dependent on the particular site of mutation. This shows that some parts of the hydrophobic cores of naturally occurring proteins are specifically and intimately packed while some parts are flexible and more tolerant to mutations. The larger the change in volume, surface area, or hydrophobicity, the more the change in stability, $\Delta\Delta G_{NU}$, seem to vary, e.g., the $\Delta\Delta G_{NU}$ of a Leu → Val mutation ranges between −0.4 and −9.4, the $\Delta\Delta G_{NU}$ of a Leu → Ala mutation between −1.7 and −24.2, and the $\Delta\Delta G_{NU}$ of a Leu → Gly mutation

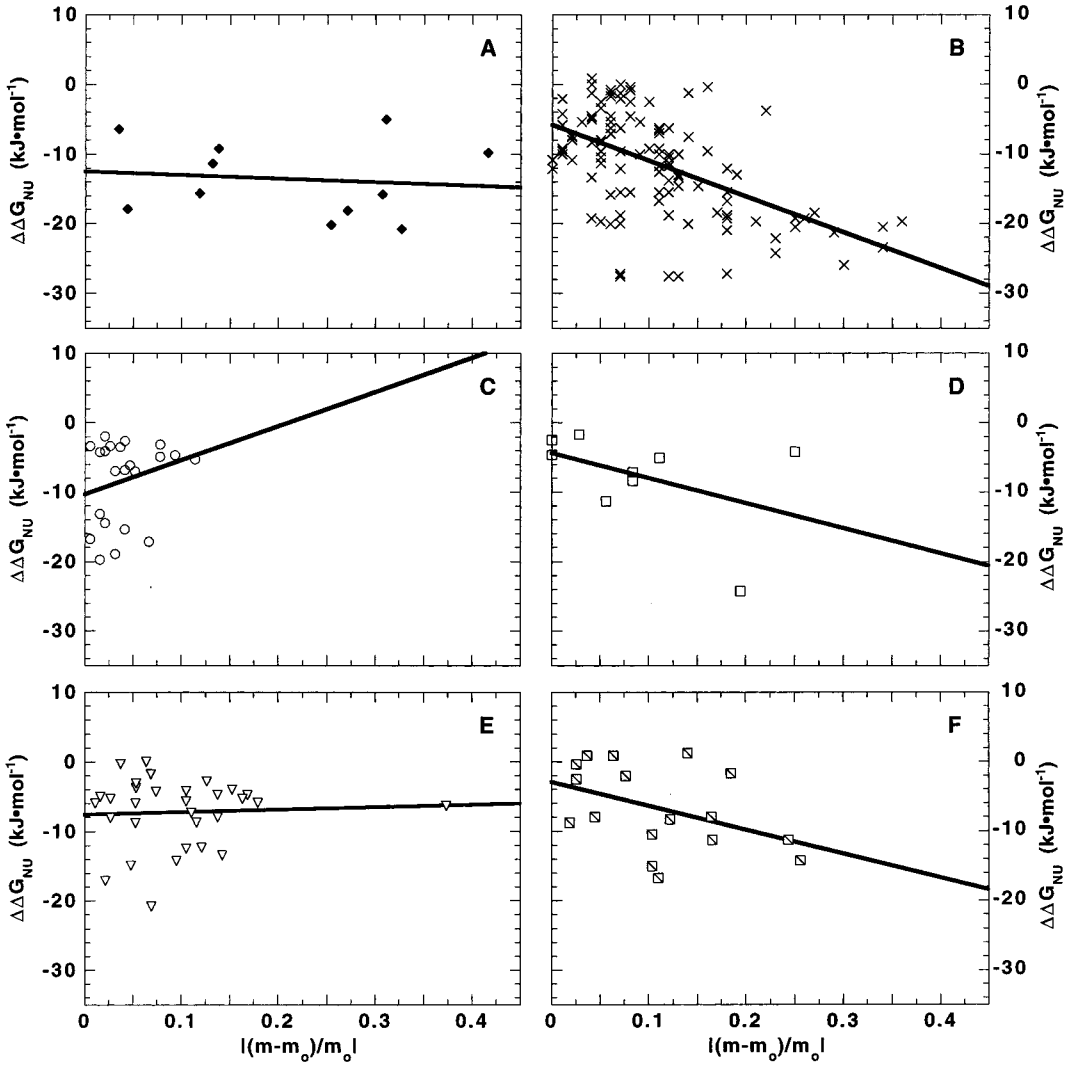

FIGURE 8: The difference in free energy of unfolding, $\Delta\Delta G_{NU}$, as a function of relative change in linear denaturant dependencies, $|\Delta m|$, between mutants and the wild-types of (A) Bovine calbindin D_{9k}, (B) *staphylococcal* nuclease, (C) barnase, (D) bacteriophage f1 gene V protein, (E) chymotrypsin inhibitor 2, and (F) bacteriophage P22 arc repressor. Symbols used are the same as in Figure 7. $\Delta\Delta G_{NU}$ is defined as $\Delta\Delta G_{NU} = \Delta G_{NU}(\text{mutant}) - \Delta G_{NU}(\text{wild-type})$. $|\Delta m|$ is defined as $|(m_{\text{mutant}} - m_{\text{wild-type}})/m_{\text{wild-type}}|$.

between −2.5 and −30.1 kJ/mol. We must not forget that some mutants may be discriminated in all possible studies due to the requirement that the mutant protein must be expressed and correctly folded. A mutant with its equilibrium shifted toward the unfolded state will be more easily degraded and difficult to obtain in its pure form. Therefore, the maximum $\Delta\Delta G_{NU}$ of mutants of a protein is governed by the ΔG_{NU} of the wild-type.

Effects on Denaturant Dependence (*m Values).* All classical theories (*67, 68*) about denaturant action come to the conclusion that m_D should be proportional to the difference between some property of the denatured state and the same property of the native state. It has been argued (*40, 69*−*71*) that changes in m are most readily explained as manifestations of changes in A_D, the solvent-accessible area of the denatured state. For *staphylococcal* nuclease, a very interesting correlation between $|\Delta m_{GuHCl}|$ and $\Delta\Delta G_{NU}$ has been shown (*40, 41*). Therefore, it was proposed that the amino sequence of wild-type *staphylococcal* nuclease has evolved to maximize the free energy of the denatured state in order to achieve a moderate level of stability. A mutation causing a stabilization of the denatured state relative to the native state would explain the observed correlation. However, no correlation between $|\Delta m|$ and $\Delta\Delta G_{NU}$ was found for calbindin D_{9k} and this led us to investigate the generality of this correlation by examining published results for barnase (*43, 44*), bacteriophage f1 gene V protein (*54*), chymotrypsin inhibitor 2 (*55, 56*), and bacteriophage P22 arc repressor (*57*) as well and compare these results with *staphylococcal* nuclease and calbindin D_{9k}. The $\Delta\Delta G_{NU}$ as a function of $|\Delta m|$ for all mutants are shown in Figure 8 together with the best-fit straight lines for each protein. It is clear that only gene V protein and arc repressor show behavior similar to *staphylococcal* nuclease, which has the most negative slope of them all. Barnase has a positive slope, whereas calbindin D_{9k} and chymotrypsin inhibitor 2 have slopes close to zero. When comparing the correlations (Table 4), similar results are obtained: *staphylococcal* nuclease has the highest correlation, followed by gene V protein and arc repressor; barnase correlation is substantially lower and the correlation factor of chymotrypsin inhibitor 2 and calbindin D_{9k} is virtually zero. Statistics show that the correlation for *staphylococcal* nuclease is highly significant (as shown previously with a different selection of mutants) with $p <$

Table 4: Linear Correlations between $|\Delta m|$ and $\Delta\Delta G_{NU}$ as Calculated by Linear Regression

	number of mutants	s[a]	correlation
calbindin D_{9k}	11	−4	0.09
staphylococcal nuclease	115	−52	0.54
barnase	22	49	0.24
gene V protein	10	−36	0.45
chymotrypsin inhibitor 2	31	4	0.05
arc repressor	17	−35	0.43

[a] Constant in the linear equation $\Delta\Delta G_{NU} = i + s|\Delta m|$.

0.001, somewhat significant for arc repressor ($p = 0.10$) and gene V protein ($p = 0.20$), and completely insignificant for the other three proteins. The *p* values are highly dependent on the number of mutants available and the possibility that a highly significant correlation would be found for other proteins if a larger number of mutants were investigated cannot be excluded, but from this set of mutants, it seems unlikely, especially for chymotrypsin inhibitor 2 and calbindin D_{9k}. It also seems unlikely that barnase would show a clear, negative slope similar to the one shown by *staphylococcal* nuclease. Thus, a correlation of $\Delta\Delta G_{NU}$ and $|\Delta m|$ indicative of a maximization of the free energy of the denatured state as seen for *staphylococcal* nuclease, is not a general feature of all proteins. This emphasizes the need to sample a large base of data for mutants of a number of different proteins when attempting to draw general conclusions about the effects of these mutations.

Thermal vs Urea Induced Unfolding. In an earlier study (*33*), the thermal unfolding of the wild-type apo calbindin D_{9k} has been studied with differential scanning calorimetry, DSC, and it was shown that the unfolding gradually took place between 60 and 100 °C with a transition midpoint of thermal denaturation, T_m, of approximately 85 °C. Even though a strict normalization of the thermal denaturation data in the present work is not feasible, it is clear that our transition midpoint, T_m, is substantially higher than 85 °C and that the thermal unfolding appears less cooperative as opposed to DSC when the unfolding is monitored by the ellipticity at 222 nm. While DSC monitors unfolding from an energetic point of view through measurements of heat capacity, ΔC_p, the ellipticity at 222 nm is a measure of the prevalence of secondary structure elements, in our case mainly α-helices. The model most consistent with these results is that the energetically important core of the protein loses its compactness first, resulting in the transitions observed by DSC. After that, the helices unfold more or less independently, as measured by ellipticity, resulting in a very uncooperative folding from a secondary structural point of view. Whether this difference in transitions gives rise to an intermediate in thermal unfolding is under investigation. What is noteworthy is the apparently different unfolding pathways depending on the denaturation method.

Conformational Effects. With respect to the question of calcium-induced structural changes and the possibility that destabilizing mutations might facilitate opening of the hydrophobic core of calbindin D_{9k}, all ANS-binding studies indicate that no such structural changes occur. Therefore, reduction of the stability of the hydrophobic core is not sufficient in and of itself to induce opening of the core upon calcium binding. With respect to the tryptophan fluorescence changes observed in the F66W mutation upon calcium binding, no other evidence from stability and ANS binding indicates structural changes. A more likely explanation for the spectroscopic changes is the large difference in dynamic properties in the apo and calcium-bound forms of calbindin D_{9k} observed previously by hydrogen-exchange studies (*72*, *73*). The more flexible apo form would be expected to allow solute oxygen in to quench the Trp fluorescence more than the rigid calcium-bound form.

CONCLUSIONS

The results presented on the stability and calcium-induced structural effects for mutants within the hydrophobic core of calbindin D_{9k} demonstrate that large alterations in stability can be tolerated by the protein while still retaining its fold and conformational response to calcium binding. The results obtained with respect to correlations of $\Delta\Delta G_{NU}$ and various physical properties of the amino acids such as surface area, volume, and hydrophobicity, are consistent with results previously obtained for other proteins and demonstrate for the first time a correlation of $\Delta\Delta G_{NU}$ and the absolute value of these properties. However, correlations with $\Delta\Delta G_{NU}$ and $|\Delta m|$ are shown to vary widely and raise doubts as to the effects of mutations on the unfolded state. These studies indicate the importance of sampling a large base of data for mutants from a number of proteins when attempting to draw general conclusions about their effects.

ACKNOWLEDGMENT

We thank Sture Forsén, Birthe B. Kragelund, and Peter Sellers for helpful discussions, and Hanna Nilsson for protein purification.

REFERENCES

1. Kragelund, B. B., Jönsson, M., Bifulco, G., Chazin, W. J., Nilsson, H., Finn, B. E., and Linse, S. (1998) *Biochemistry 37*, 8926−8937.
2. Rose, G. D. (1997) *Nat. Struct. Biol. 4* (*7*), 512−514.
3. Dalal, S., Balasubramanian, S., and Regan, L. (1997) *Nat. Struct. Biol. 4* (*7*), 548−552.
4. Cordes, M. H. J., Davidson, A. R., and Sauer, R. T. (1996) *Curr. Opin. Struct. Biol. 6* (*1*), 3−10.
5. Dill, K. (1997) *Nat. Struct. Biol. 4* (*1*), 10−19.
6. Shakhnovich, E. I. (1997) *Curr. Opin. Struct. Biol. 7* (*1*), 29−40.
7. Ho, S. P., and DeGrado, W. F. (1987) *J. Am. Chem. Soc. 109*, 6751−6758.
8. Regan, L., and DeGrado, W. F. (1988) *Science 241*, 976−978.
9. Kretsinger, R. M., and Nockolds, C. B. (1973) *J. Biol. Chem. 248*, 3313−3326.
10. Kawasaki, H., and Kretsinger, R. H. (1994) *Calcium-binding proteins*. Protein profile (Sheterline, P., Ed.) p 1, Academic Press, London.
11. Johansson, C., Brodin, P., Grundström, T., Forsén, S., and Drakenberg, T. (1991) *Eur. J. Biochem. 202* (*3*), 1283−1290.
12. Johansson, C., Ullner, M., and Drakenberg, T. (1993) *Biochemistry 32* (*33*), 8429−8438.
13. Akke, M., and Forsén, S. (1990) *Proteins: Struct., Funct., Genet. 8*, 23−29.
14. Wendt, B., Hofmann, T., Martin, S. R., Bayley, P., Brodin, P., Grundström, T., Thulin, E., Linse, S., and Forsén, S. (1988) *Eur. J. Biochem. 175*, 439−445.
15. Finn, B. E., Kordel, J., Thulin, E., Sellers, P., and Forsén, S. (1992) *FEBS Lett. 298* (*2*−*3*), 211−214.

16. Crivici, A., and Ikura, M. (1995) *Annu. Rev. Biophys. Biomol. Struct. 24*, 85−116.
17. Steiner, R. F. (1984) *Biopolymers 23* (*6*), 1121−1135.
18. Bayley, P. M., Ahlström, P., Martin, S. R., and Forsén, S. (1984) *Biochem. Biophys. Res. Commun. 120* (*1*), 185−191.
19. Brodin, P., and Grundström, T. (1986) *Biochemistry 25*, 5371−5377.
20. Johansson, C., Brodin, P., Grundström, T., Thulin, E., Forsén, S., and Drakenberg, T. (1990) *Eur. J. Biochem. 187*, 455−460.
21. Chazin, W. E., Kördel, J., Drakenberg, T., Thulin, E., Brodin, P., Grundström, T., and Forsén, S. (1989) *Proc. Natl. Acad. Sci. U.S.A. 86*, 2195−2198.
22. Aue, W. P., Batholdi, E., and Ernst, R. R. (1976) *J. Chem. Phys. 64*, 2229−2246.
23. Braunschweiler, L., and Ernst, R. R. (1983) *J. Magn. Reson. 53*, 521−528.
24. Macura, S., and Ernst, R. R. (1980) *Mol. Phys. 41*, 95−117.
25. Santoro, M. M., and Bolen, D. W. (1988) *Biochemistry 27*, 8063−8068.
26. Devore, J. L. (1982) *Probability & statistics for engineering and the sciences*, pp 447−456, Brooks/Cole Publishing Company, Monterey, CA.
27. Levitt, M. (1978) *Biochemistry 17*, 4277−4285.
28. Finn, B. E., Evenäs, J., Drakenberg, T., Waltho, J. P., Thulin, E., and Forsén, S. (1995) *Nat. Struct. Biol. 2* (*9*), 777−784.
29. Gagné, S. M., Tsuda, S., Li, M. X., Chandra, M., Smillie, L. B., and Sykes, B. D. (1994) *Protein Sci. 3*, 1961−1974.
30. Hirst, J. D., and Brooks, C. L., III (1994) *J. Mol. Biol. 243*, 173−178.
31. Chakrabartty, A., Kortemme, T., Padmanabhan, S., and Baldwin, R. L. (1993) *Biochemistry 32* (*21*), 5560−5565.
32. Woody, R. W. (1994) *Eur. Biophys. J. 23* (*4*), 253−262.
33. Linse, S., Thulin, E., and Sellers, P. (1993) *Protein Sci. 2*, 985−1000.
34. Drohat, A. C., Amburgey, J. C., Abildgaard, F., Starich, M. R., Baldisseri, D., and Weber, D. J. (1996) *Biochemistry 35* (*36*), 11577−11588.
35. Gagnè, S., Li, M., and Sykes, B. (1997) *Biochemistry 36*, 4386−4392.
36. Beckingham, K. (1991) *J. Biol. Chem. 266* (*10*), 6027−6030.
37. Evanäs, J., Thulin, E., Malmendal, A., Forsén, S., and Carlström, G. (1997) *Biochemistry 36*, 3448−3457.
38. Shortle, D. (1986) *J. Cell. Biochem. 30*, 281−289.
39. Shortle, D., Meeker, A. K., and Gerring, S. L. (1989) *Arch. Biochem. Biophys. 272*, 103−113.
40. Shortle, D., Stites, W. E., and Meeker, A. K. (1990) *Biochemistry 29*, 8033−8041.
41. Green, S. M., Meeker, A. K., and Shortle, D. (1992) *Biochemistry 31* (*25*), 5717−5728.
42. Green, S. M., and Shortle, D. (1993) *Biochemistry 32*, 10131−10139.
43. Serrano, L., Kellis, J. T., Cann, P., Matouschek, A., and Fersht, A. R. (1992) *J. Mol. Biol. 224* (*3*), 783−804.
44. Kellis, J. T., Nyberg, K., Sali, D., and Fersht, A. (1988) *Nature 333*, 784−786.
45. Hughson, F. M., Barrick, D., and Baldwin, R. L. (1991) *Biochemistry 30*, 4113−4118.
46. Lin, L., Pinker, R. J., and Kallenbach, N. R. (1993) *Biochemistry 32*, 12638−12643.
47. Pinker, R. J., Lin, L., Rose, G. D., and Kallenbach, N. R. (1993) *Protein Sci. 2*, 1099−1105.
48. Hawkes, R., Grutter, M. G., and Schellman, J. (1984) *J. Mol. Biol. 175*, 195−212.
49. Matsumura, M., Becktel, W. J., and Matthews, B. W. (1988) *Nature 334*, 406−410.
50. Karpusas, M., Baase, W. A., Matsumura, M., and Matthews, B. W. (1989) *Proc. Natl. Acad. Sci. U.S.A. 86*, 8237−8241.
51. Daopin, S., Alber, T., Baase, W. A., Wozniak, J. A., and Matthews, B. W. (1991) *J. Mol. Biol. 221*, 647−667.
52. Eriksson, A. E., Baase, W. A., Zhang, X.-J., Heinz, D. W., Blaber, M., Baldwin, E. P., and Matthews, B. W. (1992) *Science 255*, 178−183.
53. Eriksson, A. E., Baase, W. A., and Matthews, B. W. (1993) *J. Mol. Biol. 229*, 747−769.
54. Sandberg, W. S., and Terwilliger, T. C. (1991) *Proc. Natl. Acad. Sci. U.S.A. 88*, 1706−1710.
55. Jackson, S. E., Moracci, M., el Masry, N., Johnson, C. M., and Fersht, A. R. (1993) *Biochemistry 32*, 11259−11269.
56. Itzhaki, L. S., Otzen, D. E., and Fersht, A. R. (1995) *J. Mol. Biol. 254*, 260−288.
57. Milla, M. E., Brown, B. M., and Sauer, R. T. (1994) *Nat. Struct. Biol. 1*, 518−523.
58. Miller, S., Janin, J., Lesk, A. M., and Chothia, C. (1987) *J. Mol. Biol. 196*, 641−656.
59. Harpaz, Y., Gerstein, M., and Chothia, C. (1994) *Structure 2*, 641−649.
60. Guy, H. R. (1985) *Biophys. J. 47*, 61−70.
61. Kellis, J. T., Nyberg, K., and Fersht, A. R. (1989) *Biochemistry 28*, 4914−4922.
62. Arase, A., Yomo, T., Urabe, I., Hata, Y., Katsube, Y., and Okada, H. (1993) *FEBS Lett. 316*, 123−127.
63. Chen, L. H., and Baldwin, T. O. (1989) *Biochemistry 28*, 2684−2689.
64. Risse, B., Stempfer, G., Rudolph, R., Schumacher, G., and Jaenicke, R. (1992) *Protein Sci. 1*, 1710−1718.
65. Rollence, M. L., Filpula, D., Pantoliano, M. W., and Bryan, P. N. (1988) *Crit. Rev. Biotechnol. 8*, 217−224.
66. Turner, S. L., Ford, G. C., Mountain, A., and Moir, A. (1992) *Protein Eng. 5*, 535−541.
67. Schellman, J. A. (1978) *Biopolymers 17*, 1305−1322.
68. Tanford, C. (1970) *Adv. Prot. Chem. 24*, 1.
69. Shortle, D., and Meeker, A. K. (1986) *Proteins: Struct., Funct., Genet. 1*, 81−89.
70. Shortle, D., Meeker, A. K., and Freire, E. (1988) *Biochemistry 27*, 4761−4768.
71. Shortle, D., and Meeker, A. K. (1989) *Biochemistry 28*, 936−944.
72. Linse, S., Teleman, O., and Drakenberg, T. (1990) *Biochemistry 29*, 5925−5934.
73. Skelton, N. J., Kördel, J., Akke, M., and Chazin, W. J. (1992) *J. Mol. Biol. 227* (*4*), 1100−1117.
74. Skelton, J. N., Kördel, J., and Chazin, W. J. (1995) *J. Mol. Biol. 249*, 441−462.
75. Koradi, R., Billeter, M., and Wüthrich, K. (1996) *J. Mol. Graphics 14*, 51−55.

BI972642D